Optical Field Effects and Band Structure of Some Perovskite-Type Ferroelectrics

A. FROVA AND P. J. BODDY
Bell Telephone Laboratories, Incorporated, Murray Hill, New Jersey
(Received 29 July 1966)

Investigation of critical points in the band structure of some ferroelectric materials of the perovskite type has been carried out by the electroreflectance method (ER). Conducting samples of $BaTiO_3$, $KTaO_3$, and $KTaO_3$-$KNbO_3$ mixtures have been studied. The light was reflected at the interface between the samples and an electrolyte, where high electric fields could be achieved. Very large changes in the reflectivity have been measured upon application of the field. The observed behavior corresponds to shifts of the critical-point energies and splitting of the degenerate levels associated with the transition-metal–oxygen octahedra. The effect is interpreted in terms of a large lattice polarization induced by the external field. The dependence of the ER on sample orientation and light polarization has also been studied. Crystal-field symmetry considerations have allowed tentative assignments of the ER singularities to critical points in the band structure. The ER behavior in the photon range where the extinction coefficient is small compared to the refractive index is consistent with the electro-optic effect observed in the visible. It is suggested that a single mechanism accounts for both effects. In $KTaO_3$ the fundamental edge has been additionally investigated by electroabsorption. The data suggest that quantum-mechanical tunneling of the Franz-Keldysh type plays only a minor role in the optical field effects of ferroelectric crystals.

INTRODUCTION

RENEWED attention has been paid recently to the study of the fundamental properties of some ferroelectrics, especially those having perovskite-type structure. This has been motivated by the occurrence in these materials of a number of effects, such as harmonic generation[1–4] and the electro-optic effect,[5–7] which have wide applicability.[8] In addition, many of these materials can be made to conduct by doping or reduction (e.g., the transition-metal oxides), some even exhibiting superconductivity at high doping levels.[9] This has opened a whole new field of transport experiments by which to investigate their properties. Measurements such as cyclotron resonance,[10] Faraday rotation,[11] Hall and Seebeck effects,[12] and magnetoresistance[13] have provided information on the effective mass and the conduction-band minima of some of these materials.

Optical properties below the fundamental edge, such as absorption and dispersion,[14] far-infrared,[15–17] and free-carrier[18] absorption have been investigated by a number of workers. Vacuum ultraviolet reflectivity has been measured by Cardona[19] for $BaTiO_3$ and $SrTiO_3$ and by Kurtz[20] for $KTaO_3$, $KNbO_3$, and $LiNbO_3$, as well as for potassium tantalate-niobate mixtures. Assignments of the observed reflectivity peaks to critical points in the band structure have been attempted by comparison with the band structure calculated by Kahn and Leyendecker[21] in a tight binding approximation. The results of this calculation, based on a linear combination of atomic orbitals of the transition metal and the oxygen, are valid for cubic centrosymmetrical configurations and therefore are not applicable below the Curie point where cubic symmetry is destroyed or, more generally, whenever lattice polarization is present. Lifting of degeneracy at $k=0$ (Γ) points was already invoked by Casella and Keller[22] to account for the anisotropy of the absorption coefficient below the fundamental edge of barium titanate. It has been pointed out[4,8] that the strong dispersion of the electro-optic coefficients in the wavelength range near the ultraviolet could be accounted for by a large influence of electric fields on the optical transitions at energies higher than the absorption threshold. These transitions, rather than those corresponding to the fundamental gap, are responsible for the dispersion of the refractive index observed in the visible. For these reasons, field-modulated reflectance experiments (electroreflectance, referred to throughout the paper as ER) appear to be

[1] J. A. Armstrong, N. Bloembergen, J. Ducuing, and P. S. Pershan, Phys. Rev. **127**, 1918 (1962).
[2] A. Ashkin, G. D. Boyd, and L. M. Dziedzic, Phys. Rev. Letters **11**, 14 (1963).
[3] R. C. Miller, Phys. Rev. **131**, 95 (1963); Appl. Phys. Letters **5**, 17 (1964).
[4] J. F. Ward and P. A. Franken, Phys. Rev. **133**, A183 (1964).
[5] R. O'B. Carpenter, J. Am. Opt. Soc. **40**, 225 (1950).
[6] J. E. Geusic, S. K. Kurtz, T. J. Nelson, and S. H. Wemple, Appl. Phys. Letters **2**, 185 (1963).
[7] F. S. Chen, J. E. Geusic, S. K. Kurtz, J. G. Skinner, and S. H. Wemple, J. Appl. Phys. **37**, 388 (1966).
[8] J. E. Geusic, S. K. Kurtz, L. G. Van Uitert, and S. H. Wemple, Appl. Phys. Letters **4**, 141 (1964).
[9] T. F. Schooley, W. R. Hosler, and M. L. Cohen, Phys. Rev. Letters **12**, 474 (1964); M. L. Cohen, Phys. Rev. **134**, A511 (1964).
[10] L. S. Senhouse, G. E. Smith, and M. V. DePaolis, Phys. Rev. Letters **15**, 776 (1965).
[11] W. S. Baer, Phys. Rev. Letters **16**, 729 (1966).
[12] H. P. R. Frederikse, W. R. Thurber, and W. R. Hosler, Phys. Rev. **134**, A442 (1964); S. H. Wemple, *ibid.* **137**, A1575 (1965).
[13] H. P. R. Frederikse, W. R. Hosler, and W. R. Thurber, Phys. Rev. **143**, 648 (1966).
[14] For a general review of these experiments see, for example, F. Jona and G. Shirane, *Ferroelectric Crystals* (The MacMillan Company, New York, 1962).
[15] A. S. Barker, Jr. and M. Tinkham, Phys. Rev. **125**, 1527 (1962).
[16] R. C. Miller and W. G. Spitzer, Phys. Rev. **129**, 94 (1963).
[17] J. T. Last, Phys. Rev. **105**, 1740 (1957).
[18] S. Ikegamy and I. Ueda, Ann. Phys. Soc. Japan **19**, 159 (1964).
[19] M. Cardona, Phys. Rev. **140**, A651 (1965).
[20] S. K. Kurtz, T. C. Rich, and W. J. Cole (private communication).
[21] A. H. Kahn and A. J. Leyendecker, Phys. Rev. **135**, A1321 (1964).
[22] R. C. Casella and S. P. Keller, Phys. Rev. **116**, 469 (1959).

a good approach to the problem and should provide a direct correlation between band-structure and phenomenological behavior of ferroelectric materials.

In the present paper, we report such experiments for a few perovskite-type ferroelectrics. Conducting $KTaO_3$, $KTaO_3$-$KNbO_3$ mixtures, and $BaTiO_3$ have been investigated by use of liquid electrodes, the reflection occurring at a sample-electrolyte interface where large rectification barriers are present. The details of the system will be published elsewhere. Some preliminary results were previously published,[23] and a qualitative interpretation of the observed effects was given. We have extended here our investigation to the dependence of ER on crystal orientation and light polarization. Complementary electroabsorption measurements have been carried out in insulating $KTaO_3$ for a more detailed investigation of the fundamental edge. An assignment of the observed peaks to critical points in the calculated band structure is attempted and the electric-field effect is explained in terms of a shift and/or splitting of certain critical points. Discussion of the experimental results is preceded by a brief presentation of the electroreflectance method and its use to obtain band-structure information. This is followed by a description of the experimental procedure and of the sample-preparation techniques. In one section of the paper, the reflectivity modulation observed in the range of photon energies, where the extinction coefficient is zero, is correlated with the electro-optic effect measured in the visible.

I. THE ELECTROREFLECTANCE METHOD

Reflectivity measurements have been widely used in the past to investigate band structure in solids. Above the fundamental energy gap, reflectivity spectra generally show a certain amount of structure due to nonanalytic contributions to the dielectric constant coming from thresholds or saddle points in the band structure (Van Hove singularities or critical points).[24] The critical-points theory, which has been subsequently developed and extended by Phillips,[25,26] has simplified the analysis of reflectivity data to a large extent. Pseudo-potential methods have allowed successful semiempirical calculation of band structure on the basis of just a few experimental critical points.[27–29]

We recall here briefly the relationship among the parameters specifying the optical properties of a solid and their dependence on critical points in the band structure. For normal incidence, the reflectivity R is given by

$$R=\frac{(n-1)^2+k^2}{(n+1)^2+k^2}, \tag{1}$$

where n and k are, respectively, the real and the imaginary part of the refractive index. These are related to the complex optical dielectric constant ϵ^* in the well-known way. The imaginary part of the dielectric constant ϵ, due to interband contributions, is a function of frequency and is given by[25]

$$\epsilon_2(\omega)\propto\sum_{jj'}\frac{1}{\Omega}\int\frac{f_{jj'}(\mathbf{k})}{|\nabla_{\mathbf{k}}(E_{j'}-E_j)|\,(E_{j'}-E_j)}dS_{\mathbf{k}}, \tag{2}$$

where j and j' denote initial and final states, Ω is the volume of the Brillouin zone (BZ), and the integral extends over a constant interband energy defined by $E_{j'}(\mathbf{k})-E_j(\mathbf{k})=\hbar\omega$. Since the momentum matrix element $p_{jj'}\propto[f_{jj'}(E_{j'}-E_j)]^{1/2}$ can be considered to a good approximation as a constant throughout the BZ, the behavior of ϵ_2 is determined essentially by the integral

$$\frac{1}{\Omega}\int\frac{dS_{\mathbf{k}}}{|\nabla_{\mathbf{k}}(E_{j'}-E_j)|},$$

i.e., by the interband density of states. Singularity points are found in k space at those frequencies for which

$$\nabla_{\mathbf{k}}E_{j'}(\mathbf{k})-\nabla_{\mathbf{k}}E_j(\mathbf{k})=0. \tag{3}$$

At high symmetry points in the BZ, this condition can be satisfied by independent vanishing of the two terms in Eq. (3). Eq. (3), however, can be satisfied also at general points of the BZ. The above arguments apply in a similar way to the real part of the dielectric constant. The reflectivity is therefore expected to present appropriate structure in the vicinity of critical points. In practice, overlapping of ϵ_1 and ϵ_2 contributions, often from more than one critical point, lifetime broadening, and other factors have set strong limitations to the resolving power and to the sensitivity of reflectance experiments. A great improvement in this respect has been achieved by use of differential techniques, such as electroreflectance[30,31] and piezoreflectance.[32,33] In most cases, these methods have given rise to "line" spectra containing a degree of fine structure not found in absolute reflectivity. The contributions of the real and imaginary part of n^* to the modulated reflectance can be separated by differentiation of Eq. (1). One has

$$\frac{dR}{R}=\frac{4(n^2-k^2-1)dn+8nkdk}{[(n+1)^2+k^2][(n-1)^2+k^2]}. \tag{4}$$

[23] A. Frova and P. J. Boddy, Phys. Rev. Letters **16**, 688 (1966).
[24] L. Van Hove, Phys. Rev. **89**, 1189 (1953).
[25] J. C. Phillips, Phys. Rev. **104**, 1263 (1956).
[26] For a general review of optical spectra of solids and their relationship with band structure see, for instance, J. C. Phillips, in *Solid State Physics*, edited by F. Seitz and D. Turnbull (Academic Press Inc., New York, 1966), Vol. 18, p. 55.
[27] D. Brust, J. C. Phillips, and F. Bassani, Phys. Rev. Letters **9**, 94 (1962).
[28] D. Brust, M. L. Cohen, and J. C. Phillips, Phys. Rev. Letters **9**, 389 (1962).
[29] D. Brust, Phys. Rev. **134**, A1337 (1964).
[30] B. O. Seraphin and R. B. Hess, Phys. Rev. Letters **14**, 138 (1965).
[31] K. L. Shaklee, F. H. Pollak, and M. Cardona, Phys. Rev. Letters **15**, 883 (1965).
[32] W. E. Engeler, H. Fritsche, M. Garfinkel, and J. J. Tiemann, Phys. Rev. Letters **14**, 1069 (1965).
[33] G. W. Gobeli and E. O. Kane, Phys. Rev. Letters **15**, 142 (1965).

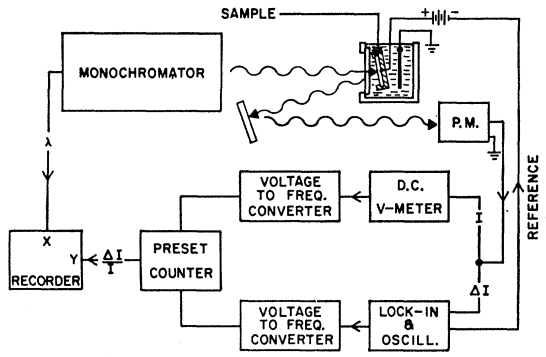

FIG. 1. Experimental apparatus.

The ratio

$$\frac{2nk}{n^2-k^2-1}=\frac{\epsilon_2}{\epsilon_1-1} \tag{5}$$

gives a measure of the relative weight of n and k in the electroreflectance (or piezoreflectance) in the various regions of the spectrum. In particular, in the region below and slightly above the fundamental edge, the electroreflectance enables one to study directly the field dependence of n (provided it is possible to apply dc fields in addition to the modulating component). This is of immediate interest in materials showing electro-optic effects in the transparent region.

Usually the Franz-Keldysh effect[34,35] (photon-assisted tunneling) almost entirely accounts for the observed ER behavior. On this basis, Aspnes[36] and Phillips[37] have recently predicted in detail the effect of electric fields at the various parabolic and saddle-point edges, thus providing a valuable assistance to the analysis of the ER spectra. As we have previously mentioned[23] and intend to discuss further in this paper, ferroelectrics appear to be an exception to the rule, since the Franz-Keldysh effect plays only a minor role in determining the size and shape of ER bands: Lattice polarization effects upset the band structure to a much larger extent and are actually responsible for the observed behavior. In the absence of a theoretical treatment of these effects, analysis of the ER structure will be carried out on the basis of a few reasonable assumptions.

II. DESCRIPTION OF EXPERIMENT

The ER was measured over a range 2 to 6.5 eV, the upper limit corresponding to the cutoff frequency of the electrolyte solution in which the sample was immersed. A block scheme of the experimental apparatus is shown in Fig. 1. Light from a high-pressure xenon discharge lamp was passed through a Spex 1500 vacuum monochromator and focused at nearly normal incidence onto the sample surface contacting the electrolyte. The reflected light was directed to an EMI-9558 QA photomultiplier. An optional polarizer (calcite Glan prism) could be inserted in the light beam just before the photomultiplier. A ratio of the dc and ac outputs of the phototube, proportional to the total and modulated reflectance, respectively, was obtained in the following way: After rectification of the ac component through lock-in detection, the two signals were converted into trains of pulses of frequency proportional to their amplitudes. The preset counter (Hewlett-Packard 5214L) counts the number of pulses received from the numerator signal during a time (gate length) which is set by the denominator signal as well as by normalizing factors. The output was finally recorded on an X-Y chart as a function of wavelength.

The small field impressing the modulation on the light was applied, along with dc fields, by biasing the sample with respect to the electrolyte. A chromium dot was evaporated in the back of the samples to provide an Ohmic contact. The samples were then encapsulated in epoxy resin with the exception of the reflecting surface. The interface between these semiconductors and an electrolyte solution behaves very similarly to a metal-semiconductor diode. In the forward direction, beyond the reversible hydrogen potential, current flows across the interface due to hydrogen evolution. In the reverse direction, there is negligible current flow up to the highest fields attained in this experiment. The solution was aqueous $M/10$ K_2SO_4, buffered to a pH value of $\sim$7.0. The voltage was applied through a platinum electrode immersed in the solution and the actual value of the bias was measured with respect to a saturated calomel reference electrode (not shown in Fig. 1). The interfacial capacitance C was measured by pulse techniques.[38] Since in these materials surface states are practically absent, the capacitance-bias relationship enabled direct determination of the surface field F_s and polarization P_s.[39] In the limit for small applied voltages, where dielectric saturation does not occur, it was possible to determine the donor density N_d from the slope of the $1/C^2$-versus-V plot. The field at the surface is then simply evaluated from $F_s=(qN_d/C_s)$, where C_s is the interfacial capacitance per unit area. The surface differential permittivity $\epsilon\epsilon_0$ at high field is given by

$$\epsilon\epsilon_0=2\left[qN_d\frac{d}{dV}\left(\frac{1}{C^2}\right)\right]^{-1},$$

and the surface polarization can be obtained from

$$P_s=\epsilon_0\int_0^{F_s}(\epsilon-1)dF_s,$$

where ϵ is a function of F_s.

[34] W. Franz, Z. Naturforsch. **13a**, 484 (1958).
[35] L. V. Keldysh, Zh. Eksperim. i Teor. Fiz. **34**, 1138 (1958) [English transl.: Soviet Phys.—JETP **7**, 788 (1958)].
[36] D. E. Aspnes, Phys. Rev. **147**, 544 (1966).
[37] J. C. Phillips, Phys. Rev. **146**, 584 (1966).
[38] W. H. Brattain and P. J. Boddy, J. Electrochem. Soc. **109**, 574 (1962).
[39] D. Kahng and S. H. Wemple, J. Appl. Phys. **36**, 2925 (1965).

It has been assumed here that N_d is constant throughout the space-charge region as well as along the surface. The latter condition is rarely ever satisfied over large areas, thus introducing a considerable error in the evaluation of the field. For this reason, field and polarization values reported in Ref. 23 may be off by as much as a factor of 2. In our subsequent experiments, we have partially overcome this difficulty by masking a portion of the sample surface and by measuring the capacitance associated with the small region where the light is focused (approximately 1×1 mm). Although a larger uncertainty has been introduced in the determination of the active area, we believe that the field has now been evaluated to within 20 or 30%.

The samples were conducting because of oxygen vacancies or impurity doping. Carrier concentration ranged between 10^{17} to 5×10^{18} per cc. The reflecting surface was obtained by cleavage, whenever this was possible [(100) surfaces of potassium tantalate and potassium tantalate-niobate]; otherwise it was etched in molten KOH or polished with 0.05 μ Linde B powder. No important differences were found among the three treatments, as was shown by comparison of $KTaO_3$ (100) surfaces prepared in the various ways.

III. POTASSIUM TANTALATE

A. Electroreflectance Results

Figures 2 and 3 show the room-temperature electroreflectance spectra for cleaved (100) and polished (111) potassium-tantalate surfaces at two different values of the dc electric field. Positive sign stands for reflectance decreasing with increasing field. Data for (110) surfaces are very similar to (111); they are shown in connection with light-polarization effects reported later in the paper. We have already pointed out[23] that the effect is at least one order of magnitude larger than in most semiconductors. For increasing fields, large shifts are observed along with the disappearance of some of the structure.

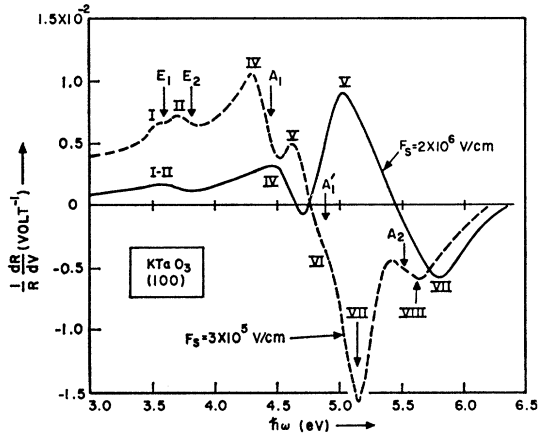

FIG. 2. ER in (100) cleaved $KTaO_3$. Donor density $N_d\simeq3.8\times10^{18}$ cm^{-3} (Ca doping).

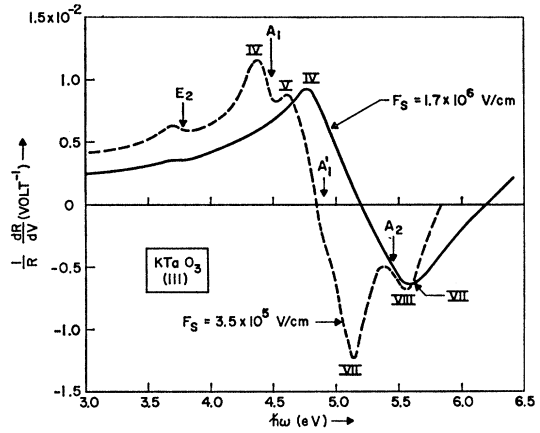

FIG. 3. ER in (111) polished $KTaO_3$. Donor density $N_d\simeq3.5\times10^{18}$ cm^{-3} (Ca doping).

It should be noted that the curves shown in Figs. 2 and 3 are somewhat related to the slope of the total-reflectivity spectra,[20] changing sign approximately at the peak of the major reflectivity band. Although some fine structure is present here that was not detected in total-reflectance measurements, we are far from having the "line" spectra associated with the Franz-Keldysh-type electroreflectance.[30] This effect should result in narrow peaks located approximately at each of the critical-point edges, the electroreflectance being practically zero at any other place. We find on the contrary that dR/dV is remarkably large even below the fundamental absorption edge (≈3.5 eV). Quantum-mechanical tunneling at the thresholds, therefore, cannot fully account for the observed behavior and one should rather think of actual displacements of the critical points.

The analysis of the curves illustrated in Figs. 2 and 3 can be made easier by comparison with a field-on–field-off total-reflectance experiment. In Fig. 4, we have shown the major R band for (100) surface at zero voltage applied (only interface-barrier field present), intermediate bias, and nearly breakdown voltage. At low field, a single peak is observed, located at 4.80 eV. When the field is increased, the peak slightly shifts to lower energy and its strength is reduced at the expense of a new band appearing on the high-energy side. The relative changes of peaks IV and V in Fig. 2 can be immediately related to this behavior. Examination of the curves of Fig. 3 leads now to the expectation that for (111) surfaces, as well as (110), such a splitting of the major reflectivity peak should not occur. Measurements of the total reflectance as a function of dc fields have indeed shown a gradual shift of the 4.80-eV band to higher energies for increasing field. This is shown in Fig. 5, where we have plotted the shift of the zero of the electroreflectance curves shown in Fig. 3—the zero occurs approximately at the reflectivity peak—versus the surface polarization P_s. The effect is larger for (111) than for (110) surfaces, but in both cases linear dependence on P_s is found. In Fig. 6, the splitting of the

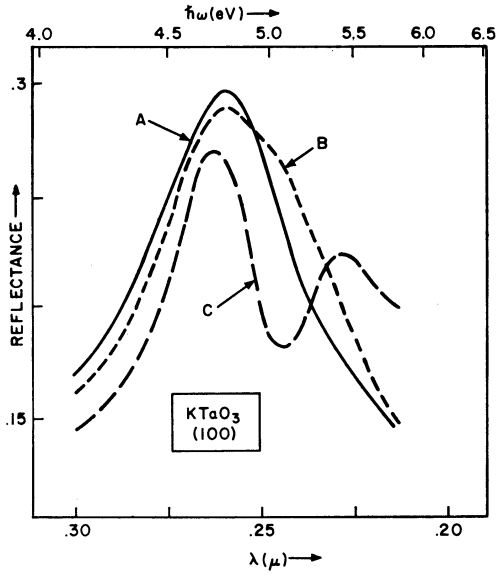

FIG. 4. Total reflectance in (100) cleaved $KTaO_3$ for three values of the surface field: 3×10^5 (A), 9×10^5 (B), and 2.6×10^6 V/cm (C).

two bands observed in (100) surfaces is shown as a function of P_s. This too has been determined from the electroreflectance spectra, being to first approximation given by the separation of the dip between peaks IV and V and the zero (Fig. 2). Data for both cleaved and etched surfaces have been plotted. No significant difference between the two treatments is visible. The (100) splitting, just as the (111) and (110) shift discussed above, is proportional to the first power of the polarization and can be as large as 0.8 eV for the largest field applied. The intercept at the ordinate is not zero, suggesting that two peaks are already present at the origin, but too closely spaced to give rise to separated bands in the total reflectance. Electroreflectance in lightly doped samples reported earlier[23] indicates that peak V is in fact present even at the lowest applied field ($\approx4\times10^4$ V/cm).

Dependence of ER on light polarization has also been

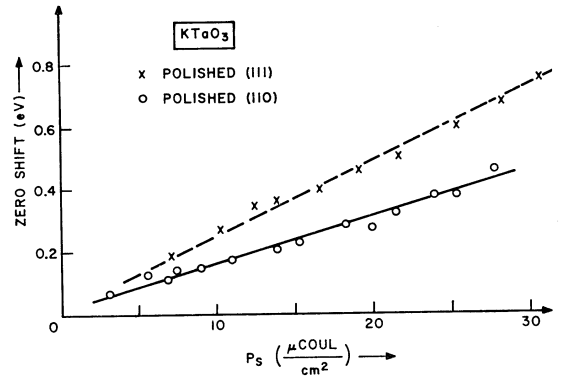

FIG. 5. Shift to higher energies of the ER zero for (110) and (111) $KTaO_3$ surfaces, as a function of surface polarization.

TABLE I. ER singularities in $KTaO_3$. Energies are given in eV.

	E_1	E_2	A_1	A_1'	A_2
$KTaO_3$ (100)	3.57	3.80	4.40	4.88	5.50
$KTaO_3$ (111)	...	3.77	4.45	4.90	5.47
$KTaO_3$ (110)	3.55	3.80	4.47	4.85	5.50

studied. Effects have been observed only in (110) surfaces, as might be expected. Figure 7 shows spectra obtained with polarization parallel to [001], [1$\bar{1}$0], and unpolarized light for one particular value of the field. On the high-energy side, data are not too accurate, owing to the high absorption of the polarizer in that range. For this field, as well as for any other field, the shift to higher energies, given by the zero displacement, and the magnitude of the modulation are approximately a factor of 2 smaller when the light is polarized along the cube edge. This is shown in Fig. 8 as a function of the surface polarization. Some saturation is seen at high fields, while at low fields a large error may be introduced by the somewhat arbitrary assumption we had to make about the initial position of the zero.

It is convenient to summarize here the results reported in this section, before proceeding to a discussion of the data and to an identification of the critical points. The energy values at which the ER singularities occur for low-surface fields have been listed in Table I for the three possible orientations of the reflecting surface. It has been assumed that the critical points, when not giving rise to transitions strong enough to cause a zero in the ER, are located at inflections between a maximum and a minimum of the ER spectrum in accordance with the arguments presented above; these points correspond approximately to shoulders in the reflectance spectrum. The following features should be stressed:

(i) For all orientations the zero of the ER is linearly shifted to higher energies for increasing surface polarization and structure is washed out; (ii) A_1 has different

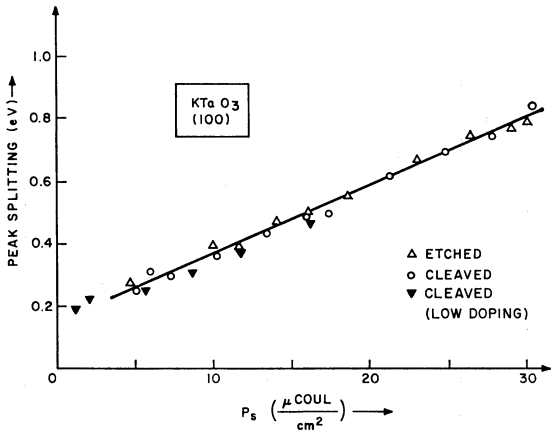

FIG. 6. Splitting of the reflectivity major peak versus surface polarization for various (100) $KTaO_3$ samples. Donor density in lightly doped material was approximately 1.5×10^{17} cm^{-3}, as opposed to $\simeq3.5\times10^{18}$ for the other two samples.

behavior for the various orientations: For increasing fields A_1 moves to slightly lower energies in (100) surfaces, while disappearing in (110) and (111) surfaces. In the (100) case this transition might actually split into two, the higher energy component getting mixed with A_1'. In the (110) surface light polarization has some effect on this critical point; (iii) for all orientations A_1' is shifted to higher energies by the field and its position is sensitive to light polarization in (110) surfaces; (iv) A_2 differs in shape for the three orientations.

B. Discussion

In Fig. 9, we show the band structure calculated for $SrTiO_3$ by Kahn and Leyendecker.[21] A picture similar to that shown in Fig. 9 should be valid for the tantalates, save for an increase in band separations because of the higher crystal fields present when Ti^{3+} is replaced by Ta^{5+}. In particular, X_2 may move higher than X_5. Inclusion of spin-orbit interaction, not considered in the calculations, should cause splittings as large as a few tenths of an eV in the tantalates. This effect is expected to be much less important in the titanates and the niobates.

We have proposed[23] that the effect of a large electric field is to displace the transition-metal ion relative to the oxygens by distances comparable to those observed when the crystal goes to its ferroelectric state.[40] This should result in changes of the Ta-O overlap integrals and shifts of the band-structure critical points. Lowering of symmetry is expected to cause lifting of degeneracy as well as changes in selection rules. In the absence of a theoretical treatment that predicts quantitatively the band-structure modifications accompanying lattice polarization, we will try to interpret the gross features of the observed ER behavior on the ground of crystal-field symmetry considerations.[41] We assume in the first approximation that the only effect of the field is to displace the Ta ion along the direction of the field

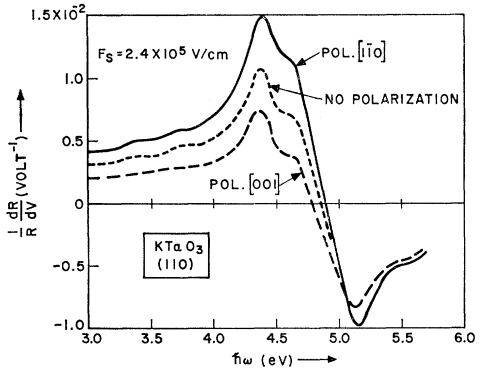

FIG. 7. Light-polarization dependence of the ER in a (110) $KTaO_3$ sample.

[40] B. C. Frazer, H. Danner, and R. Pepinsky, Phys. Rev. **100**, 745 (1955).

[41] M. Tinkham, *Group Theory and Quantum Mechanics* (McGraw-Hill Book Company, Inc., New York, 1964).

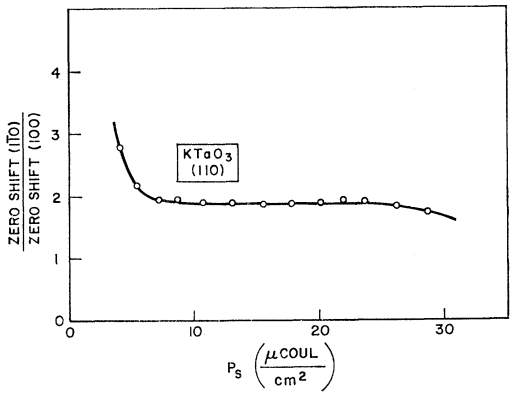

FIG. 8. Magnitude of the ER zero shift when light is polarized along [1$\bar{1}$0], relative to the shift for light polarized along the cube edge [(110) $KTaO_3$ surface].

itself, relative to the oxygens. The cubic symmetry of the crystal at zero field, O_h, is reduced to C_{4v}, C_{3v}, or C_{2v} by applying a field along [100], [111], or [110], respectively. The Brillouin zone, which is determined by the space lattice and is unaffected by the basis of atoms associated with each lattice site, remains unchanged. At the Γ point, the symmetry reduction is therefore described by the restriction of O_h to C_{4v}, C_{3v}, and C_{2v}. The three X points now no longer have the same group. For example, if the field is along [100], the symmetry at the [100] X point is described by the restriction of $D_{4h}(X)$ to $C_{4v}(\Delta)$, while the other two X points are described by the restriction of D_{4h} to $C_{2v}(Z)$. The results of this analysis can be summarized as follows:

(1) *(100) surface,* Ta *displacement and light propaga-*

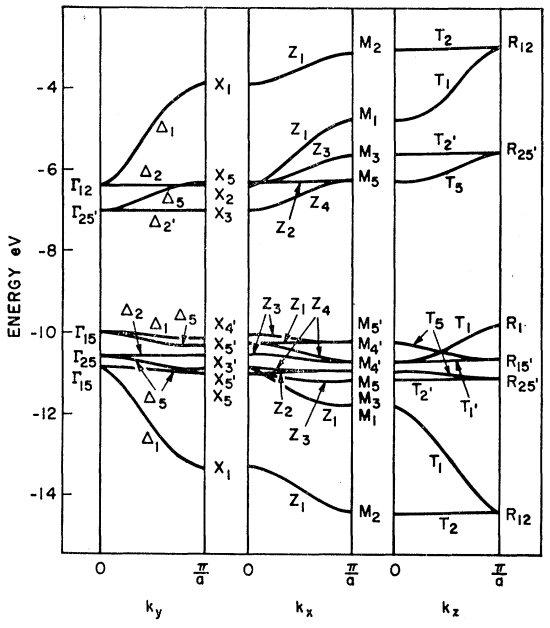

FIG. 9. Calculated band structure for perovskite-type crystals in the tight binding approximation (from Ref. 21).

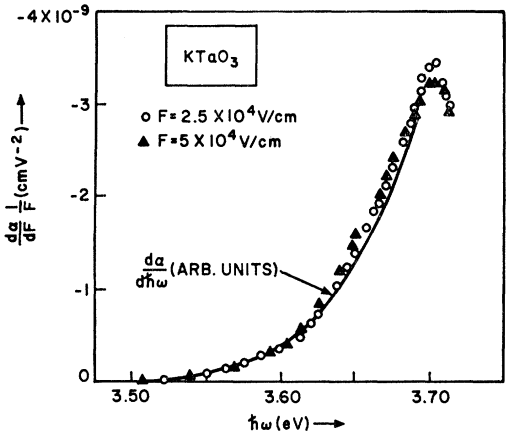

FIG. 10. Electroabsorption of $KTaO_3$ for two values of the electric field. The solid curve gives the slope of the edge.

tion along [*100*]. No polarization dependence is expected. Certain transitions at X points (such as $X_{5'} \rightarrow X_3$, $X_{4'} \rightarrow X_5$) upon application of fields give rise to two levels, one associated with the X point along [100] and the other with X points along [010] and [001]. Transitions $X_{4'} \rightarrow X_3$, $X_{3'} \rightarrow X_3$ are forbidden. Each transition at Γ points splits into two.

(2) (*111*) *surface*, Ta *displacement and light propagation along* [*111*]. No polarization dependence is expected. At X all doubly degenerate levels (e.g., $X_{5'}$ and X_5) split into two and no selection rules apply. Therefore $X_{5'} \rightarrow X_3$, $X_{4'} \rightarrow X_5$ give rise to two transitions each, $X_{5'} \rightarrow X_5$ to four. The situation is complicated by the fact that $X_{4'} \rightarrow X_3$ and $X_{3'} \rightarrow X_3$ are now allowed, owing to breaking of selection rules by the field, and they may mix with the nearby transitions. At Γ, transitions at triply degenerate points (e.g., $\Gamma_{15} \rightarrow \Gamma_{25'}$, $\Gamma_{25} \rightarrow \Gamma_{25'}$) split into three. If one of the Γ points involved is doubly degenerate (e.g., $\Gamma_{15} \rightarrow \Gamma_{12}$) only two transitions are possible.

(3) (*110*) *surface*, Ta *displacement and light propagation along* [*110*]. When light is polarized along [001], $X_{4'} \rightarrow X_3$ is allowed and gives rise to two transitions, one associated with the X point along [001] and the other with the X points along [001] and [010]. $X_{5'}$ splits, but only one $X_{5'} \rightarrow X_3$ transition is allowed. For light polarization along [$1\bar{1}0$], two $X_{5'} \rightarrow X_3$ transitions are possible, one at the [001] X point and the other at the other X points. Since both transitions occur at energies different from the $X_{5'} \rightarrow X_3$ seen with the other polarization, for unpolarized light there are five closely spaced levels instead of the initial one. Similar arguments apply to the $X_{5'}$ (lower) $\rightarrow X_3$ transition, which mixes with $X_{3'} \rightarrow X_3$ for [001] polarization. The $X_{4'} \rightarrow X_5$ transitions are affected by field identically to $X_{5'} \rightarrow X_3$. At Γ points, the $\Gamma_{15} \rightarrow \Gamma_{25'}$ splits, respectively, into three and two transitions (of different energies) with polarizations [001] and [$1\bar{1}0$].

It appears that the overlapping of so many processes whose energies and strengths are affected by field in an unknown manner renders the identification of critical points extremely difficult. It is no surprise that practically all structure disappears at even relatively low fields. We start by proposing that A_1 is in the proximity of a $X_{5'}$ (upper) $\rightarrow X_3$ transition. As discussed above, this transition should result in a large two-fold splitting for (100) surfaces, while giving rise to a higher number of close levels in the other cases. Because of the breadth of the ER bands, this structure may appear unresolved and may account for the observed disappearance of A_1 with field in (110) and (111) surfaces. Moving towards higher energies, A_1' could be assigned to a $\Gamma_{15} \rightarrow \Gamma_{25'}$ transition. We wish to point out, however, that since transitions at X should be stronger than at Γ because of their higher density of states, A_1' might well correspond to the gap between the spin-orbit split-off $X_{5'}$ and X_3. If we assign E_2 and the much weaker E_1 to a combination of indirect transitions from Γ_{15} to X_3, involving one or more phonons,[16,42] we can estimate for the energy gap a value between 3.60 and 3.80 eV: The width of the conduction band would then be of the order of 1 eV. This value is consistent with the one found from impurity-level absorption by Y. S. Chen[43] and with the magnitude of the longitudinal effective mass obtained from cyclotron resonance[10] and Faraday rotation.[11] A_2, finally, may be attributed to an $X_{5'}$ (lower) $\rightarrow X_3$ transition. Our assignments are summarized as follows:

$$E_1 = \Gamma_{15} \rightarrow X_3 \text{ (indirect)},$$
$$E_2 = \Gamma_{15} \rightarrow X_3 \text{ (indirect)},$$
$$A_1 = X_{5'} \text{ (upper)} \rightarrow X_3,$$
$$A_1' = \Gamma_{15} \rightarrow \Gamma_{25'},$$
$$A_2 = X_{5'} \text{ (lower)} \rightarrow X_3.$$

It should be pointed out that the order in which the various X transitions are encountered may actually be different. A more precise theoretical approach is needed in order for the experimental data to be completely meaningful.

C. Electroabsorption

Additional investigation of the fundamental edge has been done by observing the field-induced modulation of the transmitted light (electroabsorption). For this experiment, insulating $KTaO_3$ samples were used. The samples were lapped and polished to a final thickness of about 30 μ and were glued by silicone rubber to a wall separating two independent electrolytic cells. The side of the sample facing the wall was contacted by the electrolyte through a window previously cut in the wall itself. Dc and small ac voltages were applied between the two electrolytes. The highest dc fields that could be achieved were approximately 3×10^5 V/cm. The light was transmitted through the samples parallel to the electric field and detected by the same apparatus used

[42] A. S. Barker, Jr., Phys. Rev. 132, 1474 (1963).
[43] Y. S. Chen (private communication).

for the ER. Although this arrangement was optically very convenient, it showed a small drawback: A gradual increase in current through the sample was observed, reaching values of the order of one mA a few hours after application of the dc fields. We have attributed this behavior to the formation of hydrogen at the sample surface negatively biased with respect to the electrolyte (minimal currents may be present from the start). Hydrogen atoms subsequently diffuse through the sample and behave like donors,[44] thus lowering the resistivity of the material. The sample can be brought back to the initial condition by moderate heating.

Neglecting electroreflectance effects (approximately 5% of the total transmitted light changes in this range of photon energies) and multiple reflections, the absorption coefficient modulation per unit field, normalized to the dc applied field, is shown in Fig. 10. For the sake of clarity, data obtained for only two fields have been plotted: Results for other values of the field would nearly overlap those of Fig. 10. The sign of the effect is such that the field increases the transmission of the crystal at each wavelength. Integration of the ordinate indicates that, at each wavelength, the field-off–field-on change in the absorption coefficient α goes as the square of the electric field (or of the polarization, since ϵ is practically a constant in this range of fields). In Fig. 10 we have also plotted (solid curve) the slope of α versus $\hbar\omega$ obtained from simultaneous measurements of total transmitted light. The remarkable similarity of this curve with the field-derivative data suggests that the effect of the field is simply to displace the edge to higher energies. For an exponential edge, like the one encountered in this material, we may write

$$\alpha=\exp[\Lambda(\hbar\omega-E_0)], \tag{6}$$

where E_0 is related to the energy of the edge and $1/\Lambda$ gives a measure of its steepness. From (6) one can derive a relationship between the shift of the edge and the observed changes in absorption coefficient with field. Making use of $d\alpha=-\alpha\Lambda dE_0$, one has

$$\int_{\alpha(F)}^{\alpha(0)}\frac{d\alpha}{\alpha}=\Lambda[E_0(F)-E_0(0)]. \tag{7}$$

The edge shift, calculated from (7) at a photon energy of 3.635 eV, appears to be a function of F^2, as shown in Fig. 11. We rule out temperature modulation effects on the ground that the electroabsorption did not change during the gradual increase of the ac component of the current that we have mentioned above. Temperature effects, moreover, would result in shifts of the edge in the opposite direction. Electrostrictive strains, on the other hand, are far too small at these field values to account for the relatively large shifts observed. Normal Franz-Keldysh effect[34,35] at energies below the gap should give rise to an increase in absorption with field rather than a decrease. By analogy with the peculiar

[44] P. J. Boddy and D. Kahng (to be published).

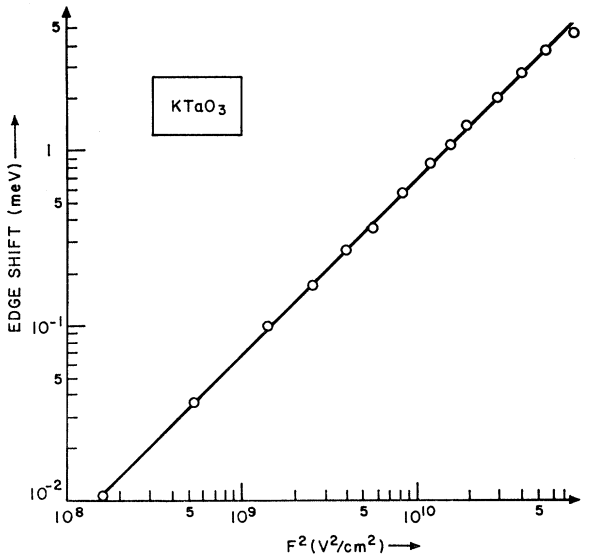

FIG. 11. Shift to higher energies of the fundamental energy gap versus the square of the applied field (from data of Fig. 10).

behavior of the ER, however, we might well expect that in ferroelectric materials the field should not only give rise to tunneling effects of the Franz-Keldysh type, but also have a direct influence on the energy gap, since it strongly affects the local fields inside the elementary cell. This effect, varying as F^2,[45] is usually of minor importance in most semiconductors. In view of a possible parallelism between this experiment and the ER, it is interesting to observe that, although the net shift of the critical points in ER varies as the first power of the field, the magnitude of the field-on–field-off modulation in certain energy ranges (e.g., from 3.5 to 4.0 eV) is proportional to F^2. At higher energies, the overlapping of all the processes discussed in Sec. IIIB may well result in an apparently incorrect field dependence. Additional experiments are needed to answer these questions. For comparison with the ER we wish to point out that the electroabsorption data of Fig. 10 present a change in slope at 3.60 eV. This coincides with the value of E_1 in the ER and seems to be the only structure present in the range of energies explored. We could not reach as high as 3.80 eV, where E_2 should be seen, but a maximum appears near 3.70 eV, just as in the ER spectrum. A more accurate investigation of the edge by electroabsorption has been undertaken with the purpose of detecting fine structure associated with the possible phonon-assisted thresholds.

D. Relationship with the Electro-Optic Effect

As discussed previously, there is a range of energies where the ER depends only upon the field-induced changes of the refractive index. The weighting factor for the separate contributions of n and k, given by Eq. (5), has been plotted in Fig. 12, using the values of

[45] E. O. Kane, J. Phys. Chem. Solids **12**, 181 (1959).

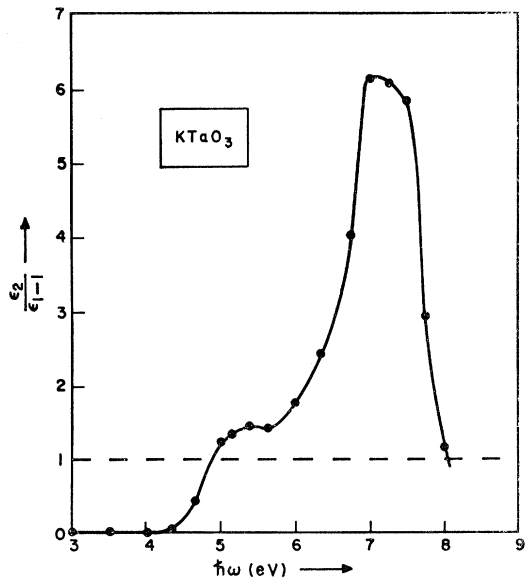

FIG. 12. Weighting factor for the separate contributions of the real and imaginary parts of the refractive index to the ER in $KTaO_3$. k becomes dominant only above 5 eV.

ϵ_1 and ϵ_2 obtained by Kurtz in reflectivity experiments.[20] It is seen that the contribution of the extinction coefficient begins to be important only above 4.25 eV. At lower photon energies, including the visible range, the ER data can be directly compared with the results of the electro-optic effect.[7,8] For the condition that the displacement D of the light be conserved normal to the surface, R variations are related to the changes of n in this direction, i.e., parallel to the applied field. In Fig. 13, we have plotted the modulated reflectance versus surface polarization at 4 eV (circles). The choice of this energy and of a lightly doped sample ($N_d \simeq 1.5\times10^{17}$ cm^{-3}) was dictated by the requirement that the penetration of the light be much smaller than the depletion layer depth, so that the effect can be to a good approximation attributed to the value of the field at the surface. From Eq. (4), for $k=0$ and including the fact that the adjacent medium has a refractive index[46] $n_0=1.356$, $(1/R)(dR/dV)=[4n_0/(n^2-n_0^2)](dn/dV)$ and upon integration, in the limit for small changes of n, one obtains the values of $\Delta n=n(0)-n(F)$ plotted in Fig. 13 (triangles).

The effect of the field is to decrease the magnitude of the refractive index by amounts proportional to the square of the polarization. From the slope of the curve of Fig. 12, $P_s^2/\Delta n$ is $\simeq 4.4\times10^{-9}$ C^2/cm^4, which corresponds to an electro-optic coefficient $g_{11}=(2/n^3)(\Delta n/P_s^2)$ of about 0.25 m^4/C^2. Although this coefficient has not been measured at energies above the gap, extrapolation of the dispersion curve of the quadratic electro-optic coefficient g_{11} in the visible, which can be obtained from Ref. 8 with reasonable approximation, shows that the above value is of the right magnitude. The data of Ref. 8 actually refer to potassium tantalate-niobate. We have made the assumption that the dispersion in $KTaO_3$ would essentially be the same save for a small translation to higher energies. Such approximations are actually not too bad, if compared to the experimental error in g_{11} ($\sim$40%) associated with the uncertainty of the field evaluation. In conclusion, the ER provides a direct determination of the electro-optic coefficients in the range of energies where transmission work is not possible. Use of insulating samples and uniform fields will enable extension of the experiment to lower energies, where the light penetration is larger, and direct comparison with the data of Ref. 8. Moreover, a variety of relative orientations of field and light beam can be chosen to determine independently the three quadratic electro-optic coefficients.

[46] *International Critical Tables* (McGraw-Hill Book Company, Inc., New York, 1930), Vol. 7, p. 13.

IV. ELECTROREFLECTANCE IN POTASSIUM TANTALATE-NIOBATE

Cleaved crystals containing approximately 35% potassium tantalate and 65% niobate were used. Such a mixture had a Curie point around 5°C and made it possible to look for changes in the ER through the transition to the ferroelectric state. The fields and the donor density could not be determined for lack of knowledge of the low-field static dielectric constant. On the other hand, because of large fluctuations in the relative concentration of the two salts, the surface polarization was far from uniform. At all applied voltages P_s was somewhat higher here than in $KTaO_3$, because of the proximity to the Curie point. In fact, large saturation of the ER occurs much earlier than in $KTaO_3$. This is shown in Fig. 14. The solid curve has been obtained with 0.5 V forward bias and the dashed

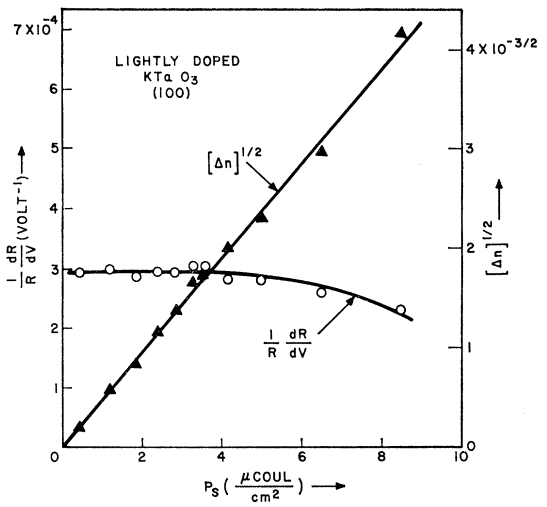

FIG. 13. ER in $KTaO_3$ (100) surface at 4 eV as a function of surface polarization (circles). The triangles show the integrated changes in the refractive index, with minus sign, due to application of the electric field.

TABLE II. ER singularities in $KTaO_3$-$KNbO_3$. Energies are given in eV.

	E_1	E_2	A_1	A_1'	A_2	B_1
$KTaO_3$-$KNbO_3$ (100)	3.60		4.15	4.55	5.15	6.10

curve with 46 V reverse. The general behavior is similar to $KTaO_3$, although some structure is missing because of the higher polarization present. Due to this fact, our critical-point values may be slightly incorrect. The observed ER singularities have been listed in Table II. All points lie about 0.2 to 0.4 eV below the corresponding $KTaO_3$ singularities. Assignments can be made, therefore, in an identical manner. B_1, which was out of the range of our experiment in $KTaO_3$, has been observed here. This critical point corresponds to the peak of the absorption coefficient[20] and could be assigned to a variety of transitions at Γ, X, or M. No appreciable change in the ER spectrum was observed when the temperature was lowered below the Curie point. We believe that the high surface field and clamping prevented the surface from undergoing ferroelectric transition. It would be worthwhile to perform the experiment with insulating material and check that the spontaneous polarization causes variations in the critical points similar to those induced by applied external fields.

V. ELECTROREFLECTANCE IN $BaTiO_3$

Ta-doped $BaTiO_3$ samples in the ferroelectric state were investigated. The reflecting surface was polished in a (100) plane in the usual way. As in potassium tantalate-niobate, saturation of the ER occurred at relatively low voltage due to the high value of ϵ. A set of spectra for increasing fields is shown in Fig. 15 (top to bottom). The observed singularities are listed in Table III and compared with Cardona's reflectivity results.[19] A_1' and A_2, which appeared there as a single maximum at the energy of A_2 (stronger than A_1'), are

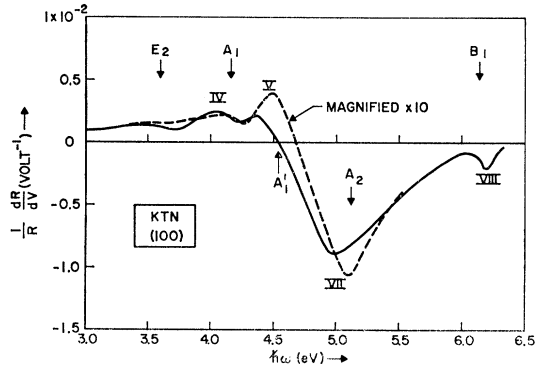

FIG. 14. ER in (100) cleaved potassium tantalate-niobate for two values of the field. Higher field data have been magnified 10 times. The sample was heavily doped by Ca impurities.

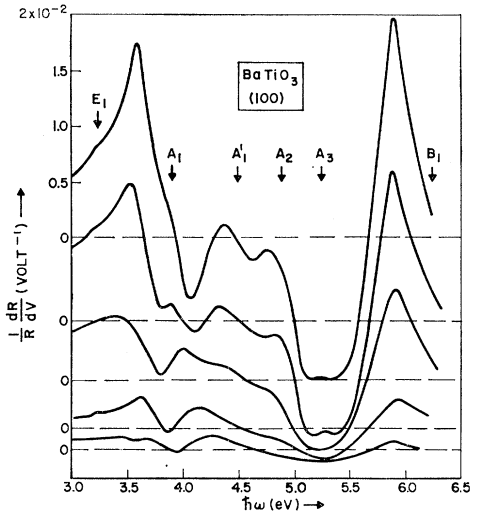

FIG. 15. ER in (100) polished $BaTiO_3$ for a number of fields (increasing from top to bottom). The samples were doped with thallium.

now clearly resolved, and A_3, previously detected in $SrTiO_3$[19] but not in $BaTiO_3$, is apparently present. Apart from this fine structure, integration with respect to $\hbar\omega$ of the lowest field ER curve yields approximately a total-reflectivity spectrum similar to that of Cardona. Starting from this curve, by use of the ER data one can reconstruct the total reflectivity at higher fields. It is seen that the major effect, in addition to general broadening of the peaks, is a change in strength and a small shift of A_1, A_2, and B_1. Assuming that transitions at X are stronger than at Γ, at least from a density-of states point of view, our assignments for $BaTiO_3$ are

$$E_1=\Gamma_{15}\rightarrow\Gamma_{25'},$$
$$A_1=X_{5'}\text{ (upper)}\rightarrow X_3,$$
$$A_1'=\Gamma_{15}\rightarrow\Gamma_{12}\text{ and/or }\Gamma_{25}\rightarrow\Gamma_{25'},$$
$$A_2=X_{5'}\text{ (lower)}\rightarrow X_3,$$
$$A_3=X_{4'}\rightarrow X_5,$$

while for B_1 a variety of transitions at X or M are possible. Once more we wish to point out that these assignments are founded upon the assumption that the order in which critical points appear in the calculated band structure[21] can be taken literally. E_1 may actually be a combination of direct and indirect transitions, since the conduction band is likely to be rather narrow.[47]

TABLE III. ER singularities in $BaTiO_3$. Data are compared with those obtained from absolute reflectivity in Ref. 19. Energies are given in eV.

	E_1	A_1	A_1'	A_2	A_3	B_1
$BaTiO_3$ (100)	3.20	3.90	4.45	4.90	5.25	~6.25
Reference 19	3.20	3.92	···	4.85	···	6.0

[47] W. S. Baer (private communication).

VI. CONCLUSIONS

The large field-induced reflectance modulation in ferroelectrics appears to be associated, at least in part, with band structure changes due to ionic displacements within the elementary cell. Because of its relationship with the electro-optic effect, usually observed in transmission, the ER stands as a complementary technique to determine the electro-optic coefficients in the regions where the material is not transparent. The ER spectra of $KTaO_3$, $KTaO_3$-$KNbO_3$, and $BaTiO_3$ present a number of singularities which have been tentatively assigned to band-structure critical points. The experimental results suggest that more theoretical knowledge of the band structure and of its changes with lattice polarization is of great necessity.

ACKNOWLEDGMENTS

The authors are very much indebted to D. Kahng for many profitable suggestions and continuous encouragement. Thanks are due to J. R. Brews for his valuable assistance in the application of symmetry arguments and to E. O. Kane for a critical reading of the manuscript. In many instances, the authors have benefited from discussions with Y. S. Chen and C. N. Berglund and from the technical assistance of W. J. Sundburg, V. J. DeLucca, and M. V. DePaolis.

PHYSICAL REVIEW VOLUME 153, NUMBER 2 10 JANUARY 1967

Single-Ion Magnetostriction in the Iron Group Monoxides from the Strain Dependence of Electron-Paramagnetic-Resonance Spectra*

T. G. PHILLIPS† AND R. L. WHITE
Stanford Electronics Laboratories, Stanford University, Stanford, California
(Received 14 July 1966)

The single-ion contribution to magnetostriction in the transition metal monoxides NiO, MnO, FeO, and CoO is calculated on a very simple model and found to account for substantially all the observed magnetostriction. Exchange is included in a molecular-field approximation, and the single-ion magnetoelastic parameters $F_{ijkl}=(\partial g_{kl}/\partial \epsilon_{ij})_0$ and $G_{ijkl}=(\partial D_{kl}/\partial \epsilon_{ij})_0$ are obtained from data on the electron paramagnetic resonance of Ni^{2+}, Mn^{2+}, Fe^{2+}, and Co^{2+} in MgO subject to uniaxial stress. Most of these data are available from the existing literature.

I. INTRODUCTION

THE linear magnetoelastic properties of magnetic materials all have their physical origin in the strain dependence of the magnetic anisotropy energy of the material. The magnetic anisotropy energy may in turn have its origin in single-ion effects which connect the spin direction of a given ion with its local crystallographic environment, or in multi-ion effects such as anisotropic exchange or dipole-dipole interactions which connect the orientation of the spins to the spatial characteristics of the spin array. We have recently shown[1] that in certain of the rare-earth iron garnets the single-ion effects are dominant in the determination of the magnetoelastic constants (specifically the magnetostriction constants) and that, further, the strain dependence of the single-ion parameters may be conveniently determined from the pressure dependence of the electron-paramagnetic-resonance spectrum of the relevant ions. We wish now to extend these ideas and arguments to the transition metal monoxides, and in particular to examine the magnetostriction constants of NiO, MnO, FeO, and CoO.

II. SPIN CONFIGURATIONS AND CRYSTALLOGRAPHIC DISTORTIONS IN THE TRANSITION METAL MONOXIDES

The transition metal monoxides NiO, MnO, FeO, and CoO all crystallize in the cubic NaCl structure and have cubic symmetry above their magnetic ordering (Néel) temperatures. Below the Néel temperature a slight distortion from cubic symmetry occurs in each case.[2–6] The magnetic order in all cases is such that the spins are ferromagnetically aligned within (111) sheets, with successive sheets antiferromagnetically aligned.[7–11] The

* Work supported in part by the Advanced Research Projects Agency through the Center for Materials Research at Stanford University and in part by the National Science Foundation through NSF Grant No. GK-202.

† Permanent address: Clarendon Laboratory, Oxford University, Oxford, England.

[1] T. G. Phillips and R. L. White, Phys. Rev. Letters **16**, 650 (1966).

[2] H. P. Rooksby, Acta Cryst. **1**, 226 (1948).
[3] N. C. Toombs and H. P. Rooksby, Nature **165**, 442 (1950).
[4] H. P. Rooksby and N. C. Toombs, Nature **167**, 364 (1950).
[5] S. Greenwald, Acta Cryst. **6**, 369 (1953).
[6] D. S. Rodbell and J. Owen, J. Appl. Phys. **35**, 1002 (1964).
[7] C. G. Shull, W. A. Strauser, and E. O. Wollan, Phys. Rev. **83**, 333 (1951).
[8] W. L. Roth, Phys. Rev. **110**, 1333 (1958).
[9] W. L. Roth, Phys. Rev. **111**, 772 (1958).
[10] W. L. Roth and G. A. Slack, J. Appl. Phys. **31**, 325S (1960).
[11] G. A. Slack, J. Appl. Phys. **31**, 1571 (1960).